



Analysis of carbonation behavior in concrete using neural network algorithm and carbonation modeling

Seung-Jun Kwon^{a,*}, Ha-Won Song^b

^a Department of Civil and Environmental Engineering, University of California, Irvine, CA 92697, USA

^b Department of Civil Engineering, Yonsei University, Seoul, 120-749, South Korea

ARTICLE INFO

Article history:

Received 30 July 2009

Accepted 26 August 2009

Keywords:

Carbonation

Modeling

Diffusion coefficient

Neural network

Porosity

ABSTRACT

Carbonation on concrete structures in underground sites or metropolitan cities is one of the major causes of steel corrosion in RC (Reinforced Concrete) structures. For quantitative evaluation of carbonation, physico-chemo modeling for reaction with dissolved CO₂ and hydrates is necessary. Amount of hydrates and CO₂ diffusion coefficient play an important role in evaluation of carbonation behavior, however, it is difficult to obtain a various CO₂ diffusion coefficient from experiments due to limited time and cost.

In this paper, a numerical technique for carbonation behavior using neural network algorithm and carbonation modeling is developed. To obtain the comparable data set of CO₂ diffusion coefficient, experimental results which were performed previously are analyzed. Mix design components such as cement content, water to cement ratio, and volume of aggregate including exposure condition of relative humidity are selected as neurons. Training of learning for neural network is carried out using back propagation algorithm. The diffusion coefficient of CO₂ from neural network are in good agreement with experimental data considering various conditions such as water to cement ratios (w/c: 0.42, 0.50, and 0.58) and relative humidities (R.H.: 10%, 45%, 75%, and 90%). Furthermore, mercury intrusion porosimetry (MIP) test is also performed to evaluate the change in porosity under carbonation. Finally, the numerical technique which is based on behavior in early-aged concrete such as hydration and pore structure is developed considering CO₂ diffusion coefficient from neural network and changing effect on porosity under carbonation.

Published by Elsevier Ltd.

1. Introduction

RC structures have undergone deteriorations due to various exposure conditions. Among the deteriorations, carbonation is one of the major deterioration phenomena in concrete in underground sites or big cities. Carbonation means deterioration leading to steel corrosion due to pH drop in pore water when concrete is exposed to CO₂ intrusion. Until the 1980s, conventional predictions for carbonation depth have been suggested with simple regression functions considering several factors such as water to cement ratio (w/c), type of binder, level of surface treatment, and environmental condition [1,2]. Recently, fundamental physico-chemo researches on carbonation behavior considering reaction with produced hydrates and dissolved CO₂ concentration are proposed [3–7]. Analysis techniques for carbonation behavior in cracked concrete as well as sound concrete are developed from qualitative macro manner [8] to quantitative micro modeling [9]. Furthermore, carbonation modeling based on behavior in early-aged concrete may be used efficiently for service life prediction of

cracked concrete structures [4,10] and permeability characteristics in carbonated concrete [11]. These models have complicated equations covering hydration of compound, dissolution and reaction of CO₂, but actually depend on diffusion coefficient of CO₂ which governs the intrusion of the mass and amount of hydration that withstands pH drop of pore water. In particular, intrusion of CO₂ is determined by diffusion coefficient so that carbonation behavior is mainly dependent on the diffusion coefficient. For reasonable evaluation of carbonation behavior, derivation of diffusion coefficients of CO₂ by experiment is essential but it is difficult to obtain them from various mixture proportions due to cost and time limitation.

Recently, a study on neural network in data processing is introduced in researches on concrete and it is very efficient compared with the simple regression analysis obtained from experimental data. However, in research field of concrete, a neural network technique is mainly applied to mixture design [12–15], strength evaluation [16,17], and reaction of hydration [18].

In this research, neural network algorithm which is mainly used in mixture design or strength evaluation is applied to analysis technique for carbonation behavior. First, estimation of CO₂ diffusion coefficient is performed through applying neural network algorithm to the previous experimental data set. Several parameters in mixture proportions and exposure condition such as water to cement ratio, unit weight of cement,

* Corresponding author. Tel.: +1 949 554 5454.

E-mail addresses: jjuni98@yonsei.ac.kr, seungjuk@uci.edu (S.-J. Kwon).

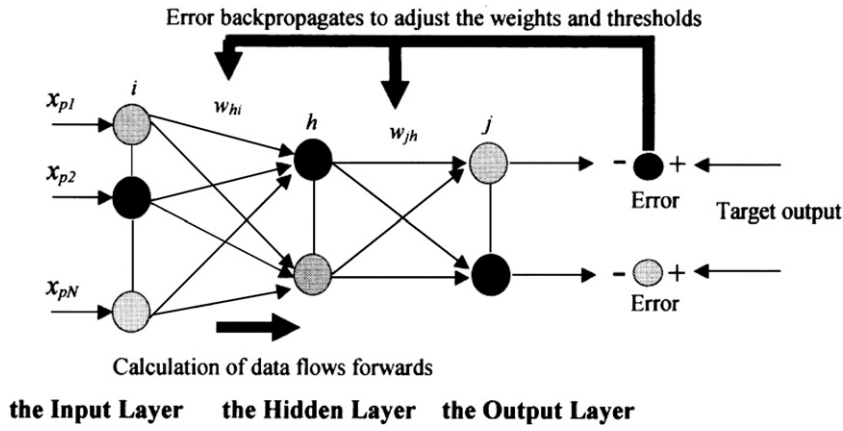


Fig. 1. Outline of simple neural network architecture [14].

volume of aggregate and sand, and relative humidity (R.H.) are selected as neurons. With selected parameters, training of learning is performed and applicability of estimated diffusion coefficient is evaluated. Second, MIP test is carried out for the evaluation of porosity change under carbonation. Then, estimated diffusion coefficients and characteristics of change in porosity are applied to carbonation analysis technique based on micro modeling, so called, multi-component hydration heat model (MCHHM) and micro pore structure formation model (MPSFM) [4,19,20]. Finally, the numerically simulated results from the proposed technique are compared with the test results and those from previous research.

2. Neural network algorithm and its application to carbonation modeling

2.1. Background of neural network

Recently, neural network algorithm is utilized for estimation of optimum value among the large data set. A neuron as unit with process of stimulus and reaction is generalized in neural network algorithm. The training for learning for set of data is performed with weight (connection strength), transfer function, and biases. The error between calculated and expected results decreases with repeating epochs and training for learning is finished when it goes down to target convergence. Simple neural network architecture has 3 layers which are composed of input, hidden, and output layers. As shown in Fig. 1, input vector $[X_p]$ has N components $[x_{p1}, x_{p2}, \dots, x_{pN}]$ and each layer is connected by weights (connection strength) $[w_{hi}, w_{jh}]$. In back propagation algorithm, value in output layer $[O_j]$ through activation function $[f]$ and threshold $[\theta_j]$ is shown in Fig. 2. Detailed information on structure of neural network can be found in previous researches [12–14].

Each input and output values should have a limit of boundary from 0.0 to 1.0 so it is necessary to perform data processing. Data processing for input and output is described as Eq. (1).

$$P_n = \frac{P_{\text{actual}} - P_{\text{min}}}{P_{\text{max}} - P_{\text{min}}} \quad (1)$$

where P_n is input value for training of learning, P_{actual} is actual input data, P_{max} and P_{min} are maximum and minimum values of a set of input data, respectively.

2.2. Application of neural network algorithm to data set

2.2.1. Test program

For measuring diffusion coefficient of CO_2 , diffusion cell and measuring equipment are generally used. In this paper, previous works [21,22] are referred for experimental data, CO_2 diffusion coefficient. The composition and characteristics of cement that were used for the diffusion measurement are shown in Table 1. Mixture design and characteristics of aggregate are listed in Table 2.

According to the researches [21,22], an equipment with diffusion cell for gas was developed, which can keep constant humidity and CO_2 concentration. Cylindrical specimens of 10 cm diameter and 20 cm height were made with the mixture proportions in Table 2 and kept in submerged condition (20 °C) for 4 weeks. After curing, the disk samples (thickness 1 cm–3 cm) from the middle of cylindrical specimens were taken and the sides were coated with epoxy for one dimensional diffusion. The samples were kept in a vacuum desiccator for obtaining a desired relative humidity based on ASTM E108-85 [23]. The steps for measurement for gas diffusion coefficient can be summarized in Table 3 including schematic drawing and CO_2 diffusion coefficient can be calculated through Eq. (2) [7].

$$D_{\text{CO}_2} = \frac{Q y_{\text{CO}_2} L}{(1 - y_{\text{CO}_2}) A} \quad (2)$$

where, D_{CO_2} is the diffusion coefficient of CO_2 , Q is the flow rate of gas, y_{CO_2} is the molar fraction of CO_2 to N_2 , L and A are thickness and area of the concrete sample. The pressure was equivalently set as 0.02 MPa for each cell and flow rate was also kept in 200 cm^3/min [21,22].

2.2.2. Obtained diffusion coefficient from neural network algorithm

In order to use neural network of back propagation, 4 input values are set up as neurons – w/c ratio, unit weight of cement, total volume ratio of sand and coarse aggregate, and exposure condition (R.H.).

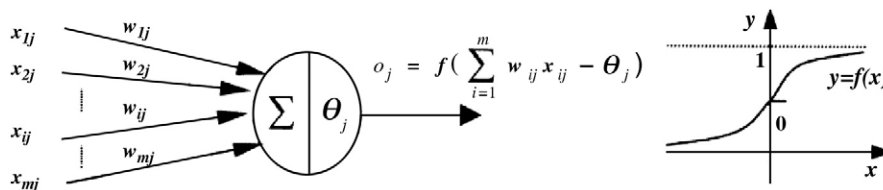


Fig. 2. Neuron's action and a sigmoid function [14].

Table 1

Composition and properties of cement [21,22].

Type	Composition (%)							Properties		
	SiO ₂	Al ₂ O ₃	Fe ₂ O ₃	CaO	MgO	SO ₃	LOI	Specific gravity	Blaine (cm ² /g)	Setting time (hour:min)
										Initial Final
Ordinary Portland cement	21.5	5.10	3.04	61.3	2.85	2.21	1.93	3.15	3,450	4:10 5:50

Table 2

Mixture proportions and characteristics of aggregate [20].

W/c ratio	Cement (kg/m ³)	Water (kg/m ³)	Fine (kg/m ³)	Coarse (kg/m ³)	Characteristics of aggregate		
0.42	425	179	714	895	Specific gravity	Absorption (%)	F. M
0.50	315	158	748	1076	Fine 2.56	2.18	2.85
0.58	277	161	726	1117	Coarse 2.60	0.94	6.51

Output value is determined as CO₂ diffusion coefficient. In data processing for input values, P_{\max} and P_{\min} are assumed as 600 and 0.0, respectively, and for output values, P_{\max} and P_{\min} are assumed as 6.0×10^{-8} and 0.0. For considering effective material components and change in diffusion coefficient with relative humidity, three components in mixture design and one exposure condition (R.H.: 10%, 45%, 75%, and 90%) are used as neurons. Tangsig function is used as transfer function and target epochs and mean square error are assumed as 1000 and 0.0001, respectively. Fig. 3 shows the comparison with the results from neural network algorithm and experiments. The maximum error between estimated and experimental data is shown to be 6.3% and reasonable agreement with results can be obtained.

2.3. Comparison with different analytical model

2.3.1. Utilized models for behavior in early-aged concrete [19]

For better understanding of this paper, the utilized micro models are briefly summarized. These models basically constitute the simulation framework of DUCOM [19] which is capable of handling the behaviors of early-aged concrete such as porosity and saturation. For analytical purpose, the interlayer porosity is simply lumped with the porosity distributions of gel and capillary porosity to obtain the total porosity distribution of cement paste as Eq. (3)

$$\phi(r) = \phi_{lr} + \phi_{cg}(r) = \phi_{lr} + \frac{1}{\phi_{cp} + \phi_{gl}} [\phi_{cp}(r) + \phi_{gl}(r)] \quad (3)$$

where r is the pore radius, ϕ_{lr} is the interlayer porosity, and ϕ_{cg} is the combined porosity distribution of capillary porosity (ϕ_{cp}) and gel porosity (ϕ_{gl}). Each of the capillary and gel porosity distribution, $\phi_{cp}(r)$ and $\phi_{gl}(r)$, are represented by a simplistic Rayleigh–Ritz (R–R) distribution function as Eq. (4).

$$V_i = 1 - \exp(-B_i r), \quad (0 \leq V(r) \leq 1), \quad dV_i = B_i r \exp(-B_i r) d \ln(r) \quad (4)$$

where V_i represents the fractional pore volume of the distribution up to the pore radius (r), and B_i is the sole porosity distribution parameter. A bimodal analytical porosity (ϕ_{total}) distribution of the cement paste can be therefore obtained as Eq. (5)

$$\phi_{total} = \phi_{lr} + \phi_{gl}[1 - \exp(-B_{gl}r)] + \phi_{cp}[1 - \exp(-B_{cp}r)]. \quad (5)$$

The distribution parameters (B_{cp} and B_{gl}) correspond to capillary and gel porosity components respectively. If the porosity is a cylindrical shape in such a distribution, then the pore distribution parameter (B_i) can be obtained from the following relationship of Eq. (6).

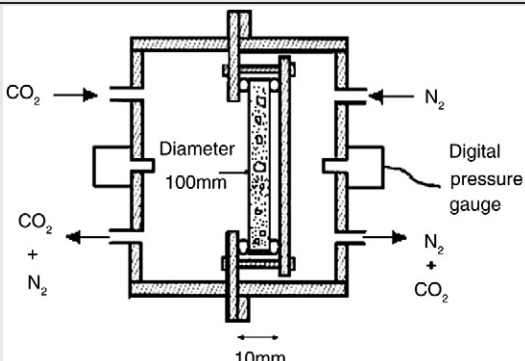
$$S_{sur} = 2\phi_i \int r^{-1} dV = 2\phi_i \int_{r_{min}}^{\infty} B \exp(-Br) d \ln(r) \quad (6)$$

Where S_{sur} is the surface area per unit volume of the matrix, r_{min} is the minimum pore radius.

Unfortunately, this expression cannot be evaluated analytically as a closed-form solution. Therefore, an explicit relationship is used, which has been obtained by fitting the accurate numerical evaluations of the above integral for a large number of data sets which relate B as a function of S_{sur}/ϕ [19]. If the porosity distribution of the microstructure is known, Eq. (7) which is derived from Kelvin's equation enables to obtain the amount of water present in the microstructure at a given ambient R.H. This is because, to satisfy the equilibrium conditions, all the pores of radii smaller than r_s would be

Table 3

Major steps for measurement of gas diffusion coefficient [21,22].

Diffusion cell for gas	Steps
	a) Installation of test equipment in room (20C) b) Measurement of concrete sample thickness and diameter c) Installation of sample (concrete disk) in cell d) Applying N ₂ gas and CO ₂ gas in different cell with same pressure e) Measurement of CO ₂ concentration when CO ₂ concentration in N ₂ gas is kept constant (steady state)

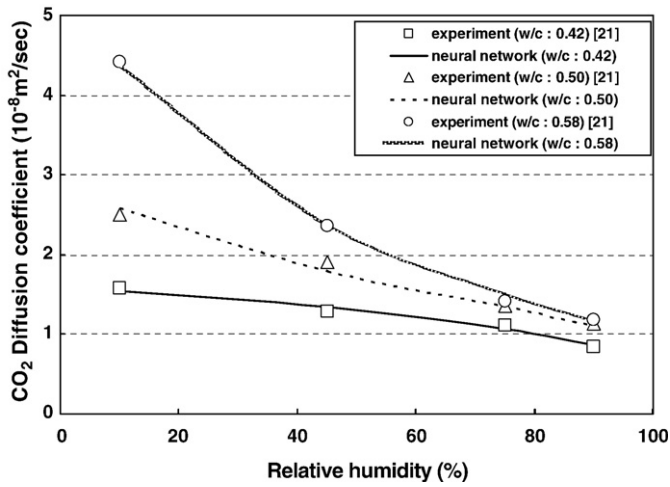


Fig. 3. Results from experiment and neural network with different water to cement ratios.

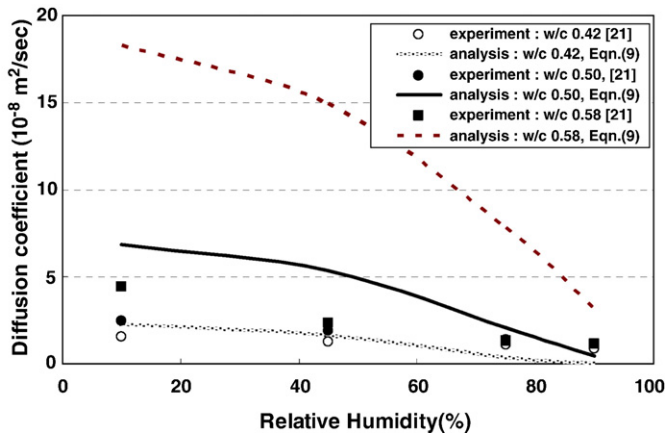


Fig. 4. Comparison with estimated results from neural network and numerical results.

completely filled whereas others would be empty. By integrating the pore volume that lies below pore radius r_s , saturation (S) can be written as the following Eq. (8) through a porosity distribution V given by Eq. (4)

$$r_s = -\frac{2\gamma M}{\rho RT} \ln(h) \quad (7)$$

where γ is the surface tension of liquid water [N/m], M_w is molecular mass of water [kg/mol], R is universal gas constant [J/mol K], T is absolute temperature [K], ρ is density of liquid water [kg/m³], h is

relative humidity of vapor phase, r_s is a pore radius [m] in which the interface is created.

$$S = \int_0^{r_s} dV = 1 - \exp(-Br_s) \quad (\text{for wetting condition}) \quad (8)$$

The expression for saturation (S) is changed with hysteretic behavior of isotherm. More detailed information considering getting stage and drying stage with trapped water are well documented in several references [4,19,20].

2.3.2. Comparison with CO₂ diffusion results

In previous researches on CO₂ diffusion [6,24], samples with cement paste are mainly used as specimen and their results of CO₂ diffusion are appeared to be higher for diffusion coefficient of concrete. Recently, models for CO₂ diffusion based on micro modeling such as porosity and saturation have been proposed [3,4,9,11]. In these researches, diffusion coefficient of CO₂ in concrete as porous media is expressed as Eq. (9) which considers both liquid diffusion in saturated pore volume and gaseous diffusion in non-saturated pore volume.

$$D_{CO_2} = \frac{\phi(1-S)^4 K_{CO_2} D_0^g}{\Omega(1+N_K)} + \frac{\phi S^4}{\Omega} D_0^d \quad (9)$$

where D_{CO_2} is the entire diffusion coefficient, ϕ is the porosity, S is saturation, K_{CO_2} is the equilibrium factor obtained from Henry's Law, Ω is the average tortuosity of a single pore ($=\pi^2/4$) which consider roughness of pore for ion movement, N_K is the Knudsen number which is the ratio of the mean free path length of a water molecule to the pore diameter. D_0^d [1.0×10^{-9} m²/s] and D_0^g [1.34×10^{-9} m²/s] are basic CO₂ diffusion coefficient in dissolved and gaseous state, respectively [3]. Unlike chloride ion transport, CO₂ transport can be explained in two states. The first term in Eq. (9) means the CO₂ diffusion in gaseous state where links of irregular paths of pores are considered. The CO₂ ion through gaseous diffusion is changed to dissolved CO₂ through multiplying equilibrium factor, K_{CO_2} where Henry's constant (H_{CO_2}) and moles of water (n_{H_2O}) are considered.

$$K_{CO_2} = \frac{1}{RT} \frac{H_{CO_2}}{n_{H_2O}} \quad (10)$$

The second term in Eq. (9) expresses the dissolved CO₂ diffusion in liquid state whose amount is determined by water capacity (ϕS).

The comparison with estimated results from neural network algorithm and numerical results from Eq. (9) is shown in Fig. 4. As shown in Fig. 4, a significant difference is evaluated in the higher w/c ratio under relatively lower relative humidity. The numerical results seem to be more sensitive to relative humidity than experimental results. The parameters in Eq. (9) are calculated through multi-component hydration heat model and micro pore structure formation model [4,9,19] which was briefly explained in Section 2.3.1.

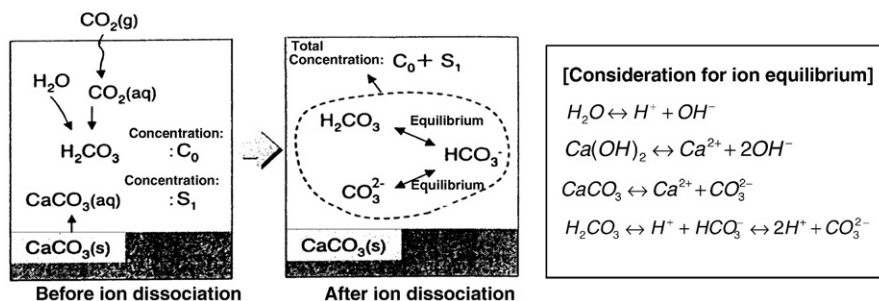


Fig. 5. Mass balance and equilibrium conditions for carbonic acid [3,9].

Table 4
Mixture proportions for MIP test and condition of accelerated carbonation.

w/c	Cement (kg/m ³)	Water (kg/m ³)	Gravel (kg/m ³)	Sand (kg/m ³)	Condition of accelerated carbonation test			
0.55	485	267	–	1353	Temp. R.H.	CO ₂ concentration	Duration period	
0.65	410	267	–	1445	25 °C 65%	5%	4 months	

3. Analysis of carbonation behavior based on neural network and micro modeling

3.1. Outline of carbonation analysis with micro modeling

Transport of ion (c_i) through porous media can be formulated as governing Eq. (11) [25].

$$\frac{\partial c_i}{\partial t} + \text{div}(J_i) + r_i = 0 \quad (11)$$

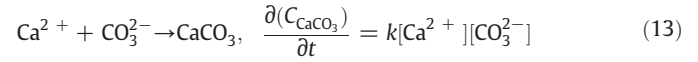
where, r_i is the reaction term accounting for complexation in the solution. For carbonation modeling, Eq. (11) can be rewritten as Eq. (12) with several parameters of porosity, saturation, and estimated diffusion coefficient ($D_{\text{CO}_2}^{\text{neural}}$) from neural network.

$$\frac{\partial}{\partial t} \{ \phi[(1-S) \cdot K_{\text{CO}_2} + S] \} \rho_d + D_{\text{CO}_2}^{\text{neural}} \nabla \rho_d - Q_{\text{CO}_2} = 0 \quad (12)$$

where, ρ_d is the dissolved CO₂ concentration, Q_{CO_2} is the sink term which is the consumption of CO₂ in unit time.

Ishida and Maekawa simply proposed the carbonation reaction with solubility of Ca(OH)₂ and CaCO₃ [3,4]. The rate of CO₂ consumption due to carbonation can be expressed by the following

differential equation as Eq. (13), assuming that the reaction is first order with respect to [Ca²⁺] and [CO₃²⁻] concentration.



where C_{CaCO_3} (mol/l) is the concentration of calcium carbonate and k (2.04 l/mol·s) is the reaction rate coefficient. For calculating a reaction rate, the relation of ion equilibriums and mass balance as shown in Fig. 5 are considered. Related ion equilibrium can be obtained as Eq. (14).

$$[\text{H}^+] + 2(S_1 + S_2) + 2S_1\alpha_0 + S_1\alpha_1 = \frac{K_w}{[\text{H}^+]} + \alpha_1 C_0 + 2\alpha_2 C_0 \quad (14)$$

Where, S_1 and S_2 are solubility of calcium carbonate and calcium hydroxide calculated by the solubility-product constant. α_0 , α_1 , and α_2 are concentration of [H₂CO₃], [HCO₃⁻], and [CO₃²⁻] in dissociated ions of CO₂ and CaCO₃. K_w is the equilibrium constant of [H⁺] and [OH⁻]. C_0 is the concentration of dissolved CO₂ (mol/l) which satisfies governing equation of Eq. (12). Eq. (14) shows that the concentration of proton [H⁺] can be obtained at an arbitrary stage as an exact solution, given the concentration of calcium hydroxide and carbonic acid before dissociation. After the concentration of protons is known, each individual ionic concentration can be calculated [3,4]. Consumed calcium hydroxide can be calculated by integrating the solubility of Ca(OH)₂ [S_2] which satisfies Eq. (14) in each time step. A detailed discussion of the carbonation reaction and carbonation process can be found in [3,4,9].

3.2. Modeling for change in porosity

During carbonation, porosity in concrete decreases due to reproduction of calcium carbonate and it leads to decrease in diffusion coefficient of CO₂ [5,6,9]. The decreasing rate and its formulation, so called decay function, are reported to be bi-linear type and it is also affected by amount of hydrates and type of cement [26,27].

3.2.1. Sample preparation

Cement mortar with two w/c ratios (0.55 and 0.65) were prepared. Each specimen was cast and stripped after 24h, cured in submerged condition for 28 days (20 °C). After curing, each specimen was kept for 2 weeks in humidity chamber at room condition (25 °C and 65% R.H.) and then accelerated carbonation test was performed. Several samples with same mixture proportions underwent longer curing period (3 months) for comparison of porosity change. As for the fully carbonated area of samples, MIP test was performed for measuring the change in porosity. The mixture design for specimen and conditions of accelerated carbonation test are shown in Table 4.

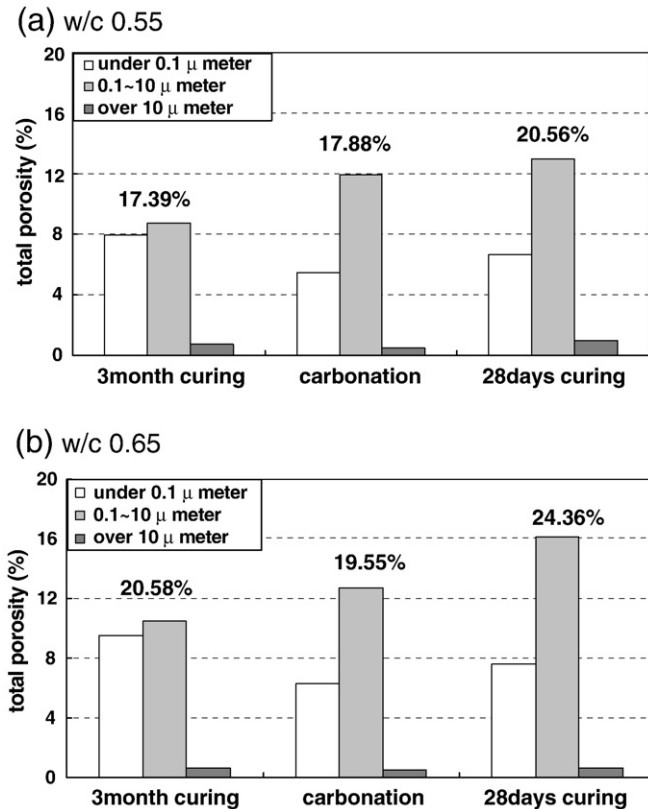


Fig. 6. Distribution in total porosity with different w/c ratios.

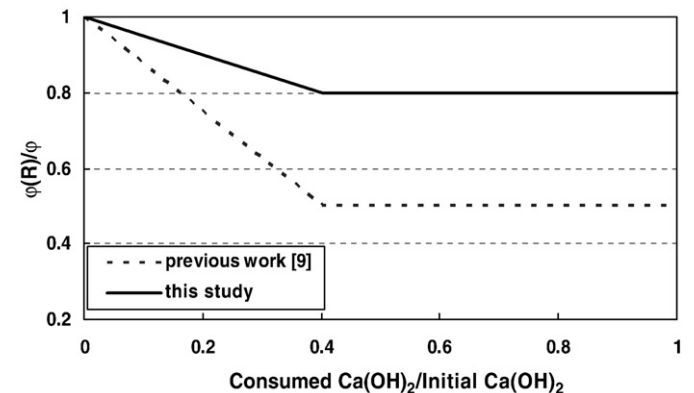


Fig. 7. Relationship between total porosity and carbonation rate.

Table 5

Terms used in governing equation for mass and energy conservation.

Variables $[X_i]$	Potential term	Flux term	Sink term
T [Temperature]	ρC [Kcal/K·m ³] – Constant	$-K_H \nabla T$ [Kcal/m ² ·s] – Constant	Q_H [Kcal/m ³ ·s] – Multi-component hydration model of cement
P [Partial vapor pressure]	$\phi \rho \frac{\partial S}{\partial p}$ [kg/Pa·m ³] – Path dependent moisture isotherms	$-(K_l + K_g) \nabla P$ [kg/m ² ·s] – Random geometry of pores and Knudsen vapor diffusion	$-Q_{hyd} - \frac{\partial(\rho S b)}{\partial t}$ [kg/m ³ ·s] – Water combined due to hydration; bulk porosity change effect
C [CO ₂ concentration]	$\phi(R)(1-S)K_{CO_2} + \phi(R)S$ [mol·l/mol·m ³] – Path dependent transport of mass – Porosity change dependent	$-\frac{\phi(R)}{\phi} D_{CO_2}^{neural} \nabla C$ [mol/m ² ·s] – Mass and Knudsen diffusion in porous media – Temperature and porosity change dependent	Q_{CO_2} [mol/m ³ ·s] – CO ₂ consumption due to carbonation process

3.2.2. MIP test

The results from porosity measurement are shown in Fig. 6. Smaller porosity in specimen with 3 month-submerged curing is measured than that in specimens with 28 day-curing. Total porosity in carbonated specimens decreases and the pore size distribution is also

changed. The porosity in specimen with 3 month curing is measured to be significantly reduced due to the sufficient curing condition, which can produce more hydrates with swelling of cement particles.

Total porosity in carbonated cement mortar of w/c 0.55 decreases to 86% of that in specimen under 28 days curing condition. In the case

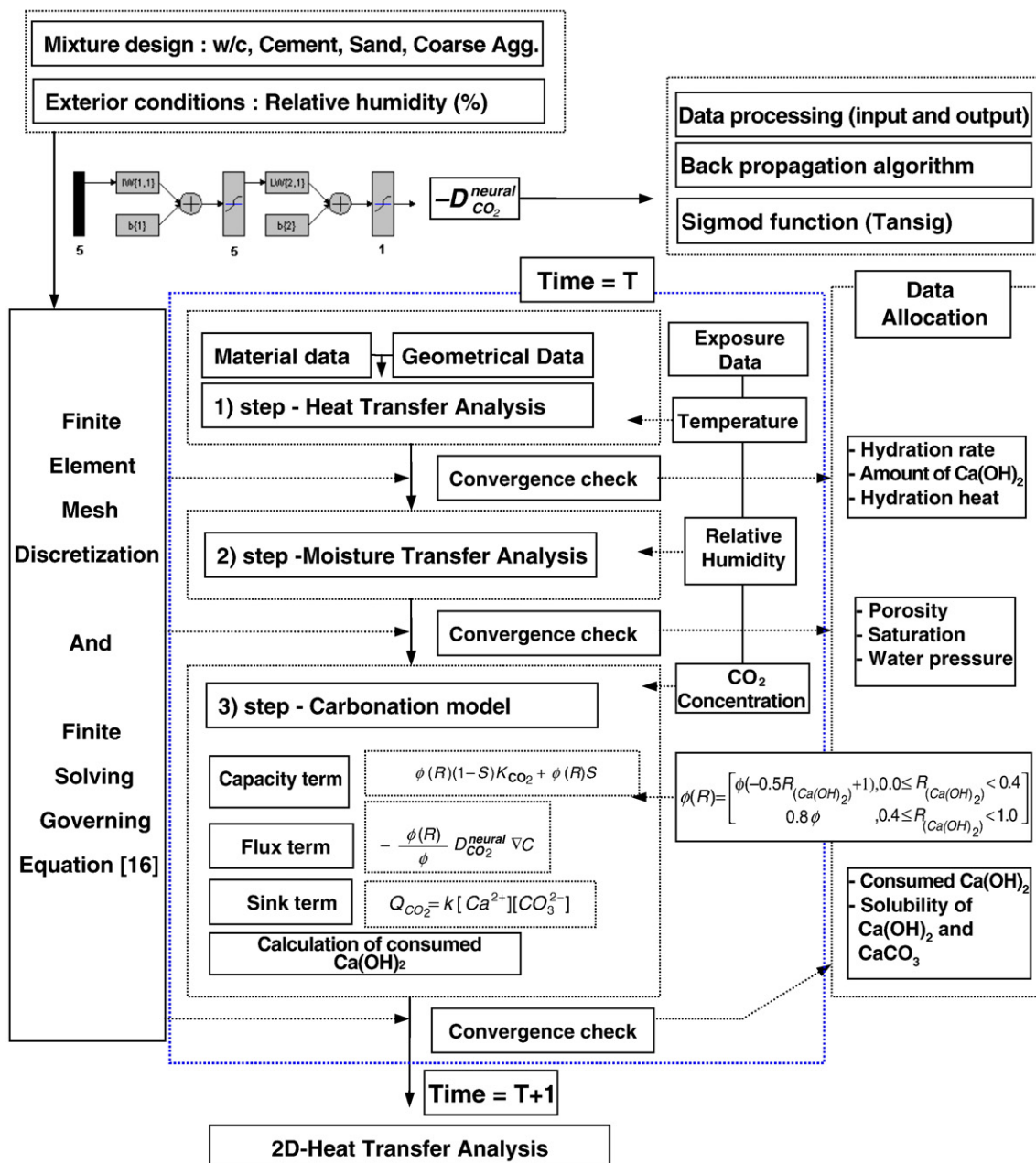


Fig. 8. Computational scheme of carbonation modeling with neural network and change in porosity.

Table 6

Estimated diffusion coefficient and condition of accelerated carbonation test.

w/c	Slump (cm)	Water (kg/m ³)	Cement (kg/m ³)	Sand (kg/m ³)	Coarse aggregate (kg/m ³ : 25 mm)	Estimated diffusion coefficient $\times 10^{-8}$ (m ² /s)
0.45	15	191	424	668	1058	1.53
0.55	15	184	335	762	1058	1.94
0.65	15	182	280	829	1041	3.33
Concentration of CO ₂		Temperature		R.H.		Exposure period
10%		25 \pm 5 °C		65 \pm 5%		4 months

of w/c 0.65, it goes down to 80% of that in initial condition. In the data of w/c 0.65, the reduction ratio to the initial condition (28 days curing) is evaluated to be less than that of w/c 0.55 but the total porosity is still greater. Since the cement mortar in w/c 0.55 has more cement amount, Ca(OH)₂ amount that is produced through hydration reaction is increased. This reproduces more CaCO₃ accordingly under carbonation and increasing volume fractile of CaCO₃ makes the pore structure of cement mortar denser as shown in Fig. 6. In this paper, the reduction ratio in porosity is assumed as 80% based on the test results. However, it is not certain when reduction of porosity starts with carbonation process. Referring to the previous research [9,27], it is reported that porosity linearly decreases and fully reduced after when the consumed Ca(OH)₂ due to carbonation is up to 40% of the initial Ca(OH)₂ amount. The formulation of decay function can be assumed as Eq. (15) and shown in Fig. 7. As described in Eq. (9), diffusion coefficient of CO₂ decreases in proportion to reduced porosity under carbonation.

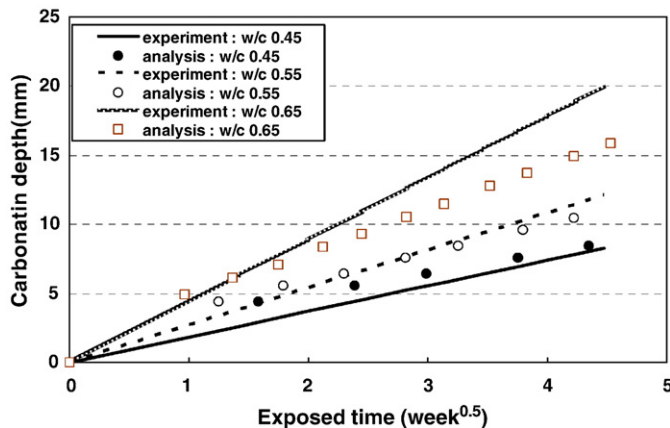
$$\phi(R) = \begin{cases} \phi(-0.5R_{\text{Ca(OH)}_2} + 1), & 0.0 \leq R_{\text{Ca(OH)}_2} < 0.4 \\ 0.8\phi, & 0.4 \leq R_{\text{Ca(OH)}_2} < 1.0 \end{cases} \quad (15)$$

where ϕ is the total porosity before carbonation, $\phi(R)$ is the total porosity under carbonation, $R_{\text{Ca(OH)}_2}$ is weight ratio (consumed calcium hydroxide due to carbonation to initial calcium hydroxide).

3.3. Numerical technique for carbonation with neural network and system dynamics

In order to simulate carbonation behavior in concrete, porosity and saturation should be obtained using governing equation for mass and energy conservation in porous media given by Eq. (16) [19].

$$\alpha_i \frac{\partial X_i}{\partial t} + \text{div} J_i(X_i, \nabla X_i) - Q_i = 0 \quad (16)$$

**Fig. 9.** Comparison with carbonation depth of simulation and experiment.**Table 7**

Different mixture proportions and condition of accelerated carbonation test.

w/c	Slump (cm)	Water (kg/m ³)	Cement (kg/m ³)	Sand (kg/m ³)	Coarse aggregate (kg/m ³ : 25 mm)	Estimated diffusion coefficient $\times 10^{-8}$ (m ² /s)
0.30	12	160	533	620	972	1.204
0.40	12	160	400	663	1038	1.597
0.50	12	185	370	647	1014	1.656
Concentration of CO ₂		Temperature		Relative humidity		Exposure period
10%		20 \pm 5 °C		60 \pm 5%		Submerged condition – 4 weeks R.H. 60% condition – 4 weeks

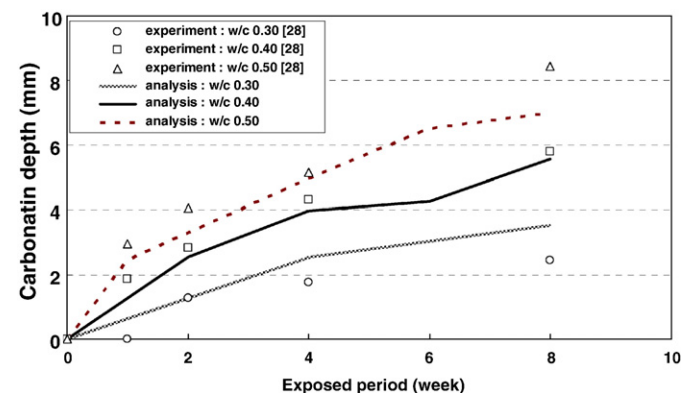
where the first is the potential term, the second is the flux term, and the last is the sink term of $[X_i]$ in Eq. (16). The details of $[X_i]$ and composition terms are explained in Table 5.

From Table 5, ρC is the specific heat capacity, K_H is the heat conductivity, Q_H is the heat generation rate, K_l and K_v are the liquid and vapor conductivities, Q_{hyd} is the combined water due to hydration [19]. For applying the result of neural network to system dynamics, $D_{\text{CO}_2}^{\text{neural}}$ is considered in the flux term with changing effect on porosity. Based on framework of FEM program DUCOM developed by the University of Tokyo [4,19], a computational scheme of carbonation modeling with neural network and changing porosity is set up as shown in Fig. 8.

In a time of T , three models are calculated successively. Through multi-component hydration heat model (MCHHM), hydration rate and amount are calculated based on stoichiometric equations. The entire specific heat generation can be explained as summation of each chemical compound – aluminate (C_3A), alite (C_3S), belite (C_2S), ferrite (C_4AF), and gypsum. Through micro pore structure formation model (MPSFM), pore structure and related moisture transport are analyzed as shown in Section 2.3.1. After convergence check of partial vapor pressure, the carbonation model is activated. Diffusion coefficient from neural network algorithm is considered and pH in pore water is determined through Eq. (14) in the carbonation model. Under carbonation process, porosity reduction rate in Eq. (15) is calculated through calculation of initial Ca(OH)₂ from hydration model and consumed Ca(OH)₂ from the carbonation model in each element.

4. Comparison with experimental and simulation results

In order to verify this proposed technique for carbonation with the neural network, accelerated carbonation test was performed. The specimens with several w/c ratios (0.45, 0.55, and 0.65) are prepared. The mixture proportions and estimated diffusion coefficient with condition of accelerated carbonation test are described in Table 6. The

**Fig. 10.** Comparison with carbonation depth of simulation and previous experiment.

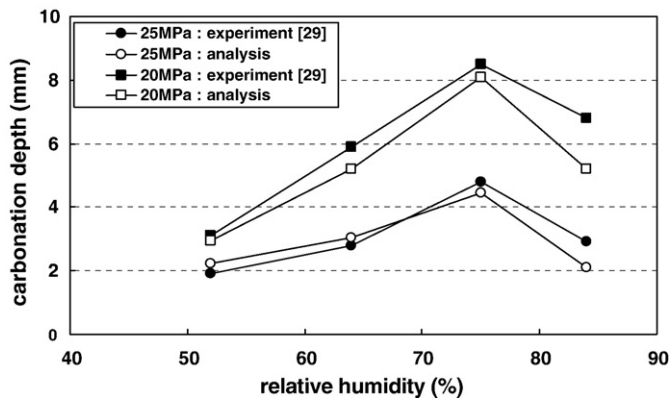


Fig. 11. Comparison with carbonation depth with different relative humidity.

simulation results show slightly an underestimation in the case of relatively higher w/c ratio (0.65) but generally, the results of simulation are in good agreement with those of experiment as shown in Fig. 9.

In addition, another data which was previously tested [28] is used for applicability of this proposed technique. The mixture proportion is shown in Table 7 with estimated coefficient and conditions of accelerated carbonation test. The comparison with experimental and numerical results is shown in Fig. 10. From the results, the proposed technique is appeared to have applicability to prediction of carbonation depth in various concrete made of ordinary portland cement (OPC).

Since carbonic reaction and CO_2 diffusion coefficient are so sensitive to saturation of pores, carbonation depth is significantly affected by the exposed relative humidity. For verification of the proposed technique, comparison of data with different relative humidity is performed. The concrete samples with 20 MPa and 25 MPa were exposed to the R.H. of 52%, 64%, 75%, and 84%. CO_2 concentration and test period were 60% and 16 weeks, respectively [29]. The comparison of results from experiment and this proposed technique is shown in Fig. 11. The difference is slightly increased in the condition of R.H. over 80%, however, the results from this technique shows reasonable agreement with the experimental data.

The proposed technique has several advantages like easy estimation of CO_2 diffusion coefficient and reasonable prediction of carbonation depth. However, the data set for neural network application have no consideration for mineral admixtures such as slag and fly ash, so that it is difficult to apply this to concrete with blended cement. Since the diffusion coefficients are obtained from constant R.H. and concentration of CO_2 , this technique may have a limited application to the RC structures with changing exterior conditions. If comprehensive data set including fineness and chemical components of cement can be utilized for acquisition of CO_2 diffusion coefficients through neural network, this proposed technique can be modified to more reliable method for predicting carbonation behavior.

5. Conclusions

The conclusions on the analysis technique for carbonation behavior in concrete using neural network algorithm and carbonation modeling are as follows.

- 1) CO_2 diffusion coefficients are estimated through neural network algorithm with 3 components in OPC mixture design and relative humidity as neurons. For 12 data set of diffusion coefficients, the results from neural network show reasonable decrease in diffusion coefficient with higher relative humidity and lower w/c ratio, with maximum difference of 6.3%.
- 2) Through the MIP test for cement mortar, decrease in total porosity under carbonation is measured to be 80–86% to initial condition. Total porosity in carbonated mortar decreases to the similar level

of that in mortar with 3-month curing under submerged condition. Even if it has 1-month curing period.

- 3) Carbonation analysis technique based on micro modeling and diffusion coefficient from neural network is proposed and it is shown to have reasonable applicability for predicting the carbonation depth in OPC concrete through comparison with results of experimental data.
- 4) With extensive and quantitative data set considering mineral admixtures, compound characteristics like fineness and replacement ratio of binder, this proposed technique based on micro modeling and neural network algorithm can be more effective for evaluation of carbonation behavior in high performance concrete as well as OPC concrete.

Acknowledgment

The authors acknowledge the financial support by a project on Standardization of Construction Specifications and Design Criteria based on Performance and the Concrete Corea Center, Korea. The coauthor of this paper, Prof. Ha-Won, Song has passed away and I would like to honor him for his contributions to this study.

References

- [1] K. Kobayashi, Y. Uno, Mechanism of carbonation of concrete, *Conc. Libr. JSCE* 16 (Dec. 1990) 139–151.
- [2] I. Izumi, D. Kita, H. Maeda, Carbonation, Kibodang Publication, 1986.
- [3] T. Ishida, K. Maekawa, Modeling of PH profile in pore water based on mass transport and chemical equilibrium theory, *Conc. Libr. JSCE* 37 (June 2001) 151–166.
- [4] K. Maekawa, T. Ishida, T. Kishi, Multi-scale modeling of concrete performance, *J. Adv. Conc. Technol.* 1 (2003) 91–126.
- [5] V.G. Papadakis, C.G. Vayenas, M.N. Fardis, Reaction engineering approach to the problem of concrete carbonation, *J. AICHE* 35 (1989) 1639–1650.
- [6] V.G. Papadakis, C.G. Vayenas, M.N. Fardis, Fundamental modeling and experimental investigation of concrete carbonation, *ACI Mater. J.* 88 (1991) 363–373.
- [7] V.G. Papadakis, C.G. Vayenas, M.N. Fardis, Physical and chemical characteristics affecting the durability of concrete, *ACI Mater. J.* 8 (1991) 186–196.
- [8] O.B. Isgor, A.G. Razaqpur, Finite element modeling of coupled heat transfer, moisture transfer and carbonation processes in concrete structures, *Cem. Conc. Compos.* 26 (Jan. 2004) 57–73.
- [9] H.-W. Song, S.-J. Kwon, K.J. Byun, C.-K. Park, Predicting carbonation in early-aged concrete, *Cem. Conc. Res.* 36 (2006) 979–989.
- [10] H.-W. Song, S.-J. Back, C.-H. Lee, S.-J. Kwon, Service life prediction of concrete structures under marine environment considering coupled deterioration, *J. Restor. Build. Monum.* 12 (4) (2006) 265–284.
- [11] H.-W. Song, S.-J. Kwon, Permeability characteristics of carbonated concrete considering capillary pore structure, *Cem. Conc. Res.* 37 (6) (2007) 909–915.
- [12] I.-C. Yeh, Modeling slump flow of concrete using second-order regressions and artificial neural networks, *Cem. Conc. Compos.* 29 (2007) 474–480.
- [13] W.P.S. Dias, S.P. Pooliyadda, Neural networks for predicting properties of concretes with admixtures, *Constr. Build. Mater.* 15 (7) (2001) 371–379.
- [14] J. Bai, S. Wild, J.A. Ware, B.B. Sabir, Using neural networks to predict workability of concrete incorporating metakaolin and fly ash, *Adv. Eng. Softw.* 34 (11–12) (2003) 663–669.
- [15] J.-Z. Wang, H.-G. Ni, J.-Y. He, The application of automatic acquisition of knowledge to mix design of concrete, *Cem. Conc. Res.* 29 (1999) 1875–1880.
- [16] J.A. Stegemann, N.R. Buenfeld, Prediction of unconfined compressive strength of cement paste with pure metal compound additions, *Cem. Conc. Res.* 32 (2002) 903–913.
- [17] I.-C. Yeh, Modeling of strength of high-performance concrete using artificial neural networks, *Cem. Conc. Res.* 28 (1998) 1797–1808.
- [18] K.B. Park, T. Noguchi, J. Plawsky, Modeling of hydration reactions using neural networks to predict the average properties of cement paste, *Cem. Conc. Res.* 35 (2005) 1676–1684.
- [19] K. Maekawa, R. Chaube, T. Kishi, Modeling of Concrete Performance: Hydration, Microstructure Formation and Mass Transport, Routledge, London, 1999.
- [20] T. Ishida, R.P. Chaube, K. Maekawa, Modeling of pore water content under genetic drying, wetting conditions, *J. JSCE* 18 (1996) 113–118.
- [21] B.H. Oh, S.H. Jung, M.K. Lee, Influence of porosity on the CO_2 diffusion characteristic in concrete, *J. KCI* 15 (2003) 778–784.
- [22] S.H. Jung, Diffusivity of carbon dioxide and carbonation in concrete through development of gas diffusion measuring system, Ph.D. dissertation, Dept. of Civil Engineering, Seoul National University, Korea, 2002.
- [23] ASTM E104–85, Standard Practice for Maintaining Constant Relative Humidity by Means of Aqueous Solution, 1996.
- [24] Y.F. Houst, F.H. Wittmann, Influence of porosity and water content on the diffusivity of CO_2 and O_2 through hydrated cement paste, *Cem. Conc. Res.* 24 (1994) 1165–1176.
- [25] F.P. Glasser, J. Marchand, E. Samson, Durability of concrete-degradation phenomena involving detrimental chemical reactions, *Cem. Conc. Res.* 38 (2008) 226–246.

- [26] T. Ishida, M. Soltani, K. Maekawa, Influential parameters on the theoretical prediction of concrete carbonation process, Proc.4th International Conference on Concrete Under Severe Conditions, Seoul, Korea, 2004, pp. 205–212.
- [27] T. Saeki, H. Ohga, S. Nagataki, Change in micro-structure of concrete due to carbonation, *Concr. Libr. JSCE* 18 (Dec. 1991) 1–11.
- [28] KICTEP, The improvement technique for quality and durability in concrete using normal and sea sand: Part 2, Quality control and evaluation of durability in concrete with sea sand, Technical Report, 1999.
- [29] S.K. Roy, K.B. Poh, D.O. Northwood, Durability of concrete-accelerated carbonation and weathering studies, *Build. Environ.* 34 (5) (1999) 597–606.